ELSEVIER

International Journal of Pharmaceutics 239 (2002) 13–22

international journal of pharmaceutics

www.elsevier.com/locate/ijpharm

Adsorption of an ionizable drug onto microspheres: experimental and modeling studies

Vincent Boudy [a,*], Nicolas Voute [b], Dominique Pradeau [c], Jean Claude Chaumeil [a]

[a] *Service Recherche et Développement, Pharmacie Centrale des Hôpitaux de Paris, 7 rue du fer à moulin, 75005 Paris, France*
[b] *BioSepra s.a, 48 avenue des Genottes, 95800 Cergy St Christophe, France*
[c] *Laboratoire Central d'Analyses, Pharmacie Centrale des Hôpitaux de Paris, 7 rue du fer à moulin, 75005 Paris, France*

Received 21 May 2001; received in revised form 9 January 2002; accepted 23 January 2002

Abstract

The purpose of this work was to study the in vitro equilibria and the adsorption kinetics of an ionizable drug, indomethacin, onto commercially available cationic polymeric microspheres: DEAE Trisacryl LS and QA Trisacryl LS. Isotherms were fitted to theoretical equations allowing accurate predictions of drug loading at different salt concentrations. Isotherm measurements were quickly obtained by simple column breakthrough experiments. The nature of the ion exchange group of the microspheres was observed to be preponderant for adsorption, as the tertiary amine derivative exhibited 53% more capacity than its quaternary amine counterpart. The maximum equilibrium uptake capacity in a 5 mM Tris–HCl buffer at pH 7.4 is 303 mmol/ml of particle volume, for DEAE microspheres. Transport properties of indomethacin into the tertiary amine microspheres were obtained in agitated contactor. Microbeads loading was completed in a 1–6 min range and was found to be controlled by pore diffusion mechanism. Equilibrium uptake data was fitted to the Langmuir and the mass action law models. Adsorption kinetics were fitted to a pore diffusion model. Good correlation was obtained between the theoretical models and the experimental data. The methodology outlined in this work provided a simple approach of estimating adsorption behavior of drugs onto ion-exchange macroporous microspheres. Although significant indomethacin loading was obtained onto the DEAE microspheres, the rapid rate of diffusion is not compatible with sustained release properties sought for this type of microspheres.

Keywords: Microspheres; Cation exchange resins; Diffusion; Adsorption

1. Introduction

Permanent embolization has been used with success for the treatment of angioma, aneuvrismal varix and arteriovenous fistula, as an alternative to surgical therapy (Djiandjian et al., 1973; Lanman et al., 1988; Biondi et al., 1990). Emboliza-

* Corresponding author. Tel.: +33-1-46-691-576; fax: +33-1-46-691-535.
E-mail address: vincent.boudy@pch.ap-hop-paris.fr (V. Boudy).

0378-5173/02/$ - see front matter
PII: S0378-5173(02)00033-9

tion can be achieved by the mechanical occlusion of the vascular lumen with particles of controlled shape and dimensions. However, recanalizations of previously occluded arteriovenous malformations have been reported (Hall et al., 1989). According to other sources, inflammation caused by the occluding materials has been identified as a major element of revascularization (Vinters et al., 1986; Thomashefski et al., 1988; Niechajev and Clodius, 1990). Therefore, embolization particles providing anti-inflammatory activity should be a promising strategy. This objective can be achieved by coupling drug release activity to the occluding property of the particle (Altman et al., 1992). A possible process to obtain such material is to reversibly adsorb ionizable drug with anti-inflammatory properties onto microspheres with ion-exchange properties that then deliver the drug with a controlled rate and target a vascular location. Ionizable drug adsorption and release onto ion-exchange matrixes have been previously studied (Farag and Nairin, 1988; Jones et al., 1989; Mohamed, 1996). However, little information is available on the mechanism of drug adsorption and drug transport within ion exchange microspheres. Moreover, there are no works that allow one to predict the quantity of bound drug on microspheres depending on the concentration of initial solution of drug and few works too that compare drug affinity for different polymers. In this study, equilibria and mass transport of indomethacin in polymer-based candidate embolization particles were investigated. The aim was to develop a model that could allow quantitative predictions and further insight into the transport mechanism. In particular, factors affecting in vitro drug loading such as counter-ion and initial drug concentrations were investigated together with intraparticle mass transport mechanisms. In this study, we used as model of embolizing particles, anion exchange resins (DEAE and QA) for their specific characteristics for embolization therapy (Beaujeux et al., 1991, 1996; Laurent et al., 1996) and as the absorbed drug, sodium indomethacin. This drug was selected both for the nature of its ionizable charge and for its potential effective action to prevent post-embolization revascularization (Altman et al., 1992).

2. Experimental section

2.1. Materials

Microspheres, DEAE Trisacryl LS (designed as DEAE microspheres) and QA Trisacryl LS (designed as QA microspheres) were obtained from BioSepra s.a. (Cergy Saint Christophe, France). These resins were originally designed as chromatographic media for biomacromolecule purification. These materials are hydrophilic macroporous ion-exchangers prepared as spherical semi-rigid microbeads of 80–160 μm diameter with a mean diameter of 120 μm. They are obtained by free radical polymerization in a w/o emulsion system of cationic acrylic derivatives with a hydrophilic acrylic monomer and are crosslinked with a hydroxylated acrylic bifunctional monomer. The ionizable groups are strong quaternary amines for the QA resin and a 70/30 mixture of weak tertiary amines and strong quaternary amines for the DEAE resin. The intraparticle porosity of the ion-exchangers is 69% of the bead volume. The interparticle porosity of a packed bed of microspheres is 35% of the bed volume. By strict control of the polymerization conditions, a macroporosity is obtained with an exclusion molecular weight limit of the microsphere pore of approximately 10^7 Da.

2.2. Solute

Sodium indomethacin (MW = 433, $pK_a = 4.5$) was supplied by Merck Sharp & Dohme-Chibret (Rahway, USA). Solutions of concentrations 0.325–5.20 g/l were obtained by dissolving appropriate amounts in 5 mM Tris–HCl pH 7.4 buffer. Indomethacin was fully soluble in the range of concentration investigated.

2.3. Column experiments

Equilibrium isotherm was measured using column assays. The column adsorption experiments were carried out with a 6.6 mm i.d., 100 mm length glass column, a peristaltic pump and a UV detector equipped with a flow through cell. The output of the UV detector was recorded with

a strip chart recorder. The temperature was maintained at 25 °C. Column effluent volumes were accurately measured by collecting the column outlet into a burette. After column packing, the resin was equilibrated with 20 column volumes of 5 mM Tris–HCl pH 7.4 buffer. Then, an indomethacin solution with a defined concentration was loaded onto the column at a superficial velocity of 210 cm/h. Solute concentration at the column outlet was continuously detected by UV adsorbance at 410 nm. This wavelength was selected as it allows linear detection of the indomethacin concentration in the studied range. The loading was stopped when the column outlet concentration of indomethacin was equal to the stock solution concentration. The equilibrium capacity of the column microspheres was determined from the experimental column breakthrough curve.

At equilibrium, the amount of solute held into the column is equal to the surface area above the breakthrough curve and can be determined with the following equation:

$$Q = C_0 V_b - \int_0^{V_b} C(v)\,dv \quad (1)$$

where Q is solute held in the column; C_0, solute concentration in the feed; C is solute concentration in the column effluent; V_b is volume for which $C = C_0$.

With the assumption of a sigmoid shape for the breakthrough profile, Eq. (1) can be simplified as follows:

$$Q = C_0 V_{50\%} \quad (2)$$

where $V_{50\%}$ is volume at which $C = 0.5 \times C_0$.

The solute concentration in the microsphere phase ($\bar{C}$) in equilibrium with the feed stock concentration C_0 is then found with Eq. (3).

$$\bar{C} = \frac{Q - Q_0 - Q_p}{V_c(1 - \varepsilon_0)} \quad (3)$$

where Q_o is the amount of solute held in the system void volume (including tubing volume and dead zone in the column headers and UV measurement cell); Q_p is the amount of solute held in the total porosity of the column; V_c is the column volume; and ε_0 is the interparticle porosity.

The amount of solute held in the system void volume and column porosity can be washed out by a cleaning step with pure buffer. The total porosity (ε_T) of the column corresponds to the bead interparticle porosity (ε_0) and the bead intraparticle porosity ε_p.

$$\varepsilon_T = \varepsilon_0 + (1 - \varepsilon_0)\varepsilon_p \quad (4)$$

The frontal chromatography technique described above was also used for the measurement of total ion exchange capacity of the microspheres. In this situation, the solute was a 0.1 M HCl solution. The conductivity of the column effluent was continuously measured and recorded. Prior to the measurement the column was regenerated with 5 column volume of 1 M NaOH and rinse with distilled water. The total ion capacity of the resin was determined with Eq. (3).

2.4. Batch experiments

Measurement of adsorption kinetics was performed in a 500 ml agitated contactor. Indomethacin concentration in solution was monitored by continuously recirculating a stream through a UV spectrophotometer, equipped with an analytical cell and a peristaltic pump. Residence time in the measurement loop was minimized. The stream was drawn through a stainless steel frit to prevent recirculating beads in the loop. At the start of the experiment, the vessel was filled with an appropriate volume of a solution (50–200 ml) at a given concentration (0.65–2.60 g/l). The experiment was started when ca. 1 ml of microspheres equilibrated with the buffer and superficially dried was quickly introduced into the vessel. The UV signal was recorded on a strip chart recorder and converted to concentration through a calibration curve. The temperature was maintained at 25 °C. The amount of solute adsorbed by the media at each time was obtained by the following mass balance equation:

$$\bar{C}(t) = \frac{(C_0 - C(t))}{H} \quad (5)$$

where $\bar{C}(t)$ is the amount of solute adsorbed per unit volume of particle at t time; H is microsphere volume to liquid phase volume ratio; and $C(t)$ is solute concentration in the liquid phase at t time.

Titration of a 8.5 ml of DEAE microspheres previously regenerated with 1 N NaOH, extensively rinsed with distilled water and resuspended in 40 ml of 0.5 M KCl was performed with 100 mM HCl.

3. Results and discussion

3.1. Equilibrium of adsorption

The adsorption results of indomethacin onto DEAE and QA microspheres are shown on Figs. 1 and 2.

Two approaches were used to model the solute uptake by the ion-exchange resins: the mass action model and the Langmuir formalism. As shown below, both approaches lead to a unique mathematical expression, in the case of a univalent solute, as the indomethacin.

The mass action model (MA) represents the solute ion-exchange adsorption process as a stoichiometric exchange of liquid phase solute and bound counterions (Whitley et al., 1989). The uptake is given by:

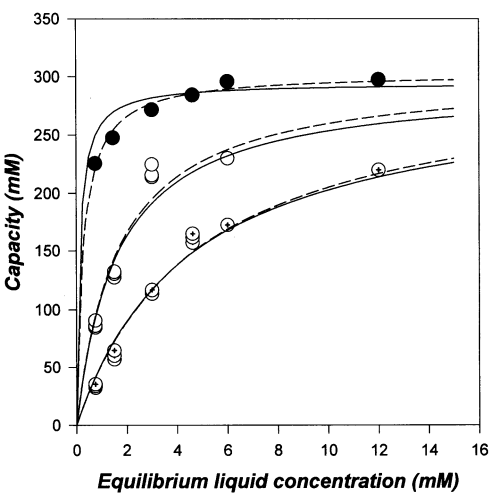

Fig. 1. Equilibrium uptake of indomethacin on DEAE microspheres in 5 mM Tris–HCl buffer pH 7.4 at different counterion concentrations: 4.2 mM (closed circles); 50 mM (open circle); 140 mM (crossed circles). Dotted lines represent predictions of the Langmuir model with parameters in Table 1. Continuous lines represent the mass action model with parameters in Table 3.

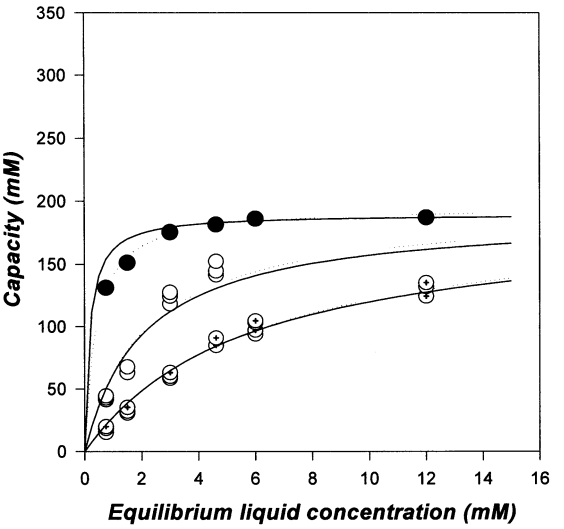

Fig. 2. Equilibrium uptake of indomethacin on QA microspheres in 5 mM Tris–HCl buffer pH 7.4 at different counterion concentrations: 4.2 mM (closed circles); 50 mM (open circles); 140 mM (crossed circles). Dotted lines represent predictions of the Langmuir model with parameters in Table 2. Continuous lines represent the mass action model with parameters in Table 3.

$$ {}_{\beta}\mathrm{R}_{\mathrm{esin}}\mathrm{C}_{\mathrm{counterion}} + \mathrm{S}_{\mathrm{olute}} \rightleftarrows \mathrm{R}_{\mathrm{esin}}\,{}_{\beta}\mathrm{S}_{\mathrm{olute}} + {}_{\beta}\mathrm{C}_{\mathrm{counterion}} $$

where β is the effective charge of the solute, which is pH dependent. The counterion is assumed to be monovalent.

The apparent equilibrium constant of the ion exchange process is defined as:

$$ K_{\mathrm{eq}} = \left(\frac{\overline{C}}{C}\right)\left(\frac{I}{\overline{I}}\right)^{\beta} \tag{6} $$

where C, I are the solute and counterion concentrations in the liquid phase, and $\overline{C}$, $\overline{I}$ the concentrations in the microsphere phase.

Unlike strong cationic resin, the number of ionizable groups on the weakly cationic resin is related to the pH and the total number of charges by the Henderson–Hasselbach relationship:

$$ \mathrm{pH} = \mathrm{p}K_{\mathrm{a}} + \log\left(\frac{\gamma}{1-\gamma}\right) \tag{7} $$

where γ is the degree of ionization of the resin.

However, some of charged groups are not available for exchange with the solute due to a steric hindrance effect as the solute can not diffuse into the narrower pores.

The number of charged groups on the resin sterically excluded from exchange is given by:

$$\hat{I} = \alpha\Lambda \tag{8}$$

where Λ is the ionic capacity of the resin (total number of charge/unit volume of bead) and α, the size exclusion fraction.

When the interface equilibrium is reached the total number of counterions adsorbed to the support is given by:

$$I_t = \hat{I} + \bar{I} \tag{9}$$

with I_t is the total number of counterions adsorbed per unit volume of resin and $\bar{I}$ is the number of counterions adsorbed and available for exchange.

A consequence of this model is that unbound solute can only interact with unhindered ion-exchange sites.

Electroneutrality on the microsphere phase requires:

$$\Lambda = \hat{I} + \bar{I} + \beta\overline{C} \tag{10}$$

Combining Eqs. (6) and (10) and Eq. (8) gives:

$$\overline{C} = K_{eq} C \frac{(\Lambda(1-\alpha) - \beta\overline{C})^{\beta}}{I^{\beta}} \tag{11}$$

This equation defines a single component isotherm, based on the mass action law.

It should be pointed out that a numerical method is required to calculate the solute microsphere phase concentration, for a given liquid phase concentration. Competitive multicomponent isotherm can be formulated as a simple extension of the single component equilibrium. Moreover steric hindrance of counterion by adsorbed large macromolecules can be included in the mass action formalism (Brooks and Cramer, 1992).

When the solute characteristic charge is one, the MA model may be rearranged to form a Langmuir expression:

$$\bar{C} = \frac{\Lambda(1-\alpha)\dfrac{K_{eq}}{I} C}{1 + \dfrac{K_{eq}}{I} C} \tag{12}$$

where the maximum capacity is defined as $\bar{C}_{max} = \Lambda(1-\alpha)$ and the association constant

$$K_L = \frac{K_{eq}}{I},$$

Eq. (12) can be found directly by assuming a second-order kinetics binding process.

$$S_{olute} + L_{igand} \underset{k_{des}}{\overset{k_{ads}}{\rightleftarrows}} S_{olute}L_{igand} \tag{13}$$

where S_{olute} is the solute, L_{igand} the ligand, $S_{olute}L_{igand}$ the complex and where k_{ads}, k_{des} are the association and dissociation rate constants, respectively.

The rate equation for the second-order kinetics is given by Eq. (14)

$$\frac{d\bar{C}}{dt} = k_{ads}\ C(\bar{C}_{max} - \ \bar{C}) - k_{des}\bar{C} \tag{14}$$

where $\bar{C}$and C are the solute concentrations in the microsphere and liquid phase, respectively, and $\bar{C}_{max}$ the maximum solute binding capacity.

At equilibrium $d\bar{C}/dt = 0$ and thus Eq. (14) yields the Langmuir isotherm:

$$\bar{C} = \frac{\bar{C}_{max} K_L C}{1 + K_L C} \tag{15}$$

with

$$K_L = \frac{k_{ads}}{k_{des}}$$

is dependent on the temperature, the pH and the composition of the liquid phase.

The data on Figs. 1 and 2 were fitted to the Langmuir model, Eq. (15), by a least squares procedure based on the Marquardt–Levenberg method (Marquardt, 1963). This approach is more robust than Scatchard plots, the semi-reciprocal plot or the double inverse plot that are susceptible to introduce experimental uncertainty into the independent variables (Johnson and Faunt, 1992). Estimated parameters for Eq. (15) as well as standard errors are reported in Table 1. The maximum amount of indomethacin adsorbed by the tertiary amine ion exchanger is 55% higher than the uptake of the quaternary amine resin. The apparent dissociation constant, defined as $K_d = 1/K_L$, is dependent on the counter ion concentration. Within the range of concentration in-

Table 1
Langmuir equilibrium parameters for the adsorption of indomethacin on DEAE microspheres at different counterion concentrations

Counterion (mM)	$\bar{C}_{max}$ (mM)	S.E.	K_L (mM^{-1})	S.E.
4.2	303	4.2	3.55	0.41
50	303	30.9	0.60	0.14
140	303	22.6	0.21	0.03

vestigated the correlation between K_d and I is linear as shown on Fig. 3. As expected for ion exchangers an increase of the counterion concentration increases the dissociation constant of the equilibrium. For any counterion concentration, the QA microspheres exhibit a lower affinity for indomethacin compared to the DEAE microspheres. At the minimum counterion concentration (4.2 mM) the apparent dissociation constant is lower on the tertiary amine ion exchanger: 282 μM compared to 383 μM for the DEAE and QA microspheres respectively. The affinity for the resins is weak and will permit significant solute release under physiological conditions.

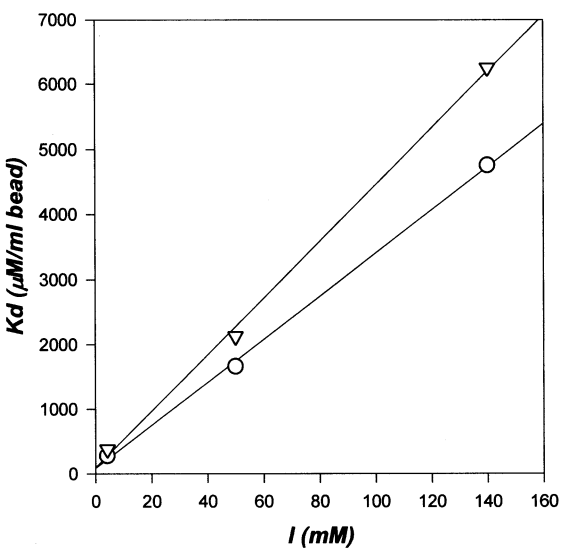

Fig. 3. Correlation between the apparent dissociation constant K_d and the counterion concentrations. Uptake of indomethacin on QA microspheres in 5 mM Tris–HCl buffer pH 7.4 at (open triangles). Uptake of indomethacin on DEAE microspheres in 5 mM Tris–HCl buffer pH 7.4 (open circles).

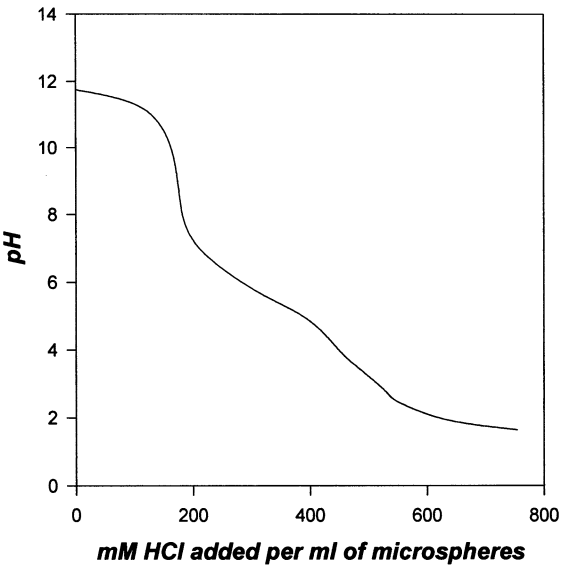

Fig. 4. Plot of the pH titration curves of DEAE microspheres (titration of 8.5 ml of DEAE microspheres by a 100 mM HCl. Microspheres regenerated with 1 N NaOH, rinsed with distilled water and resuspended in 0.5 M KCl).

Using Eq. (15), C can be calculated from the quantity of drug desired at the target location, namely $\bar{C}$.

The data were also used to fit the mass action model, Eq. (12). This model requires the determination of the total ion exchange capacity of the microspheres. It was measured using frontal chromatography with a 100 mM HCl titration solution. The total numbers of charged groups based on the bead volume are 267 and 517 mM, for QA resin and DEAE resin respectively. For the quaternary amine ion exchanger, the number of ionizable groups is equivalent to the total number of charged groups. However, for the tertiary amine resin the number of ionizable groups depended on the pH, therefore a correction to the total ionic capacity was made using Eq. (7). Titration curves for DEAE microspheres is shown on Fig. 4. It indicates the presence of two basic groups with a pK_a value of 6.7 for 70% of the immobilized charges and a pK_a of 10.7 for the remaining 30% of immobilized charges. With these data, the calculated number of charged groups at pH 7.4 is 341 mM.

Table 2
Langmuir equilibrium parameters for the adsorption of indomethacin on QA microspheres at different counterion concentrations

Counterion (mM)	$\bar{C}_{max}$ (mM)	S.E.	K_L (mM^{-1})	S.E.
4.2	196	2.4	2.61	0.22
50	196	25.3	0.47	0.14
140	196	10.6	0.16	0.02

Best fit parameter estimates for Eq. (12) are reported in Table 3 and the fitted curves are shown in Figs. 1 and 2. Excellent agreement is found between the experimental data and the model. Contrary to the Langmuir isotherm, the effect of the counterion is explicitly accounted for in the mass action model. Therefore, it can be used to predict the effect of the increase in counterion concentration on the uptake isotherm.

The difference of indomethacin binding capacity of the two ion exchangers can be explained on one hand by the difference in the concentration of immobilized charges on each resin, and on the other hand, by a higher steric hindrance factor for the quaternary amine microspheres compared to the tertiary amine microspheres. This latter factor may be explained by a higher crosslinking of the QA hydrogel resulting in a lower accessibility of the narrower pores.

From the equilibrium results, it can be concluded that the DEAE microspheres is the most suitable microsphere for the binding of indomethacin as it exhibits a higher binding capacity as well as a lower dissociation constant. The Langmuir model and the Mass action model provide an equally good fit of the data. However, the mass action model is preferable as it includes explicitly the impact of the counterion concentration. A set of adjusting parameters is required for each counterion concentration with the Langmuir model.

Table 3
Mass action law parameters for the adsorption of indomethacin on DEAE and QA microspheres

Microspheres	Λ (mM)	α	K_{eq}
DEAE microspheres	341.00	0.136	30.92
QA microspheres	267.00	0.289	24.14

3.2. Kinetics of adsorption

Experimental results from indomethacin stirred batch adsorption kinetics onto DEAE microspheres are shown on Fig. 5. The experimental points shown are taken from a continuous chart recorder trace rather than being individual measurements.

Numerous reports indicate that, for ion exchangers, the kinetics of binding is much faster than the rate of diffusion (Ruthven et al., 1984). Therefore, mass transfer in an ion exchanger can be only affected by two types of resistances in series: external film mass transfer resistance and intraparticle mass transfer resistance (LeVan et al., 1997). Two types of intraparticle mass transfer have been described: homogeneous particle diffusion (transport by diffusion of solute in the adsorbed state or solid diffusion) and pore diffusion (transport by diffusion through the liquid contained in the pores of the particle). Pore diffusion occurs when the pore size of a liquid filled pore particle is large in comparison to the mean free path of the solute molecule (Li et al., 1995). This situation provided an accurate description of the system under study for which the ratio of the pore diameter to the solute free path was large.

An analytical solution of the mass transport equation for pore diffusion alone was found for the case of very favorable isotherms assuming a finite fluid volume. The time needed to attain a certain fractional approach to equilibrium is given by (Theo and Ruthven, 1986):

$$\frac{\varepsilon_p D_p C_0 t}{r^2 \bar{C}_\infty} = I_2 - I_1 \tag{16}$$

where

$$I_1 = \frac{1}{6\lambda R}\ln\left(\frac{\lambda^3+\eta^3}{\lambda^3+1}\left(\frac{\lambda+1}{\lambda+\eta}\right)^3\right) + \frac{1}{\lambda R\sqrt{3}}\left(\tan^{-1}\left(\frac{2\eta-\lambda}{\lambda\sqrt{3}}\right) - \tan^{-1}\left(\frac{2-\lambda}{\lambda\sqrt{3}}\right)\right) \tag{17}$$

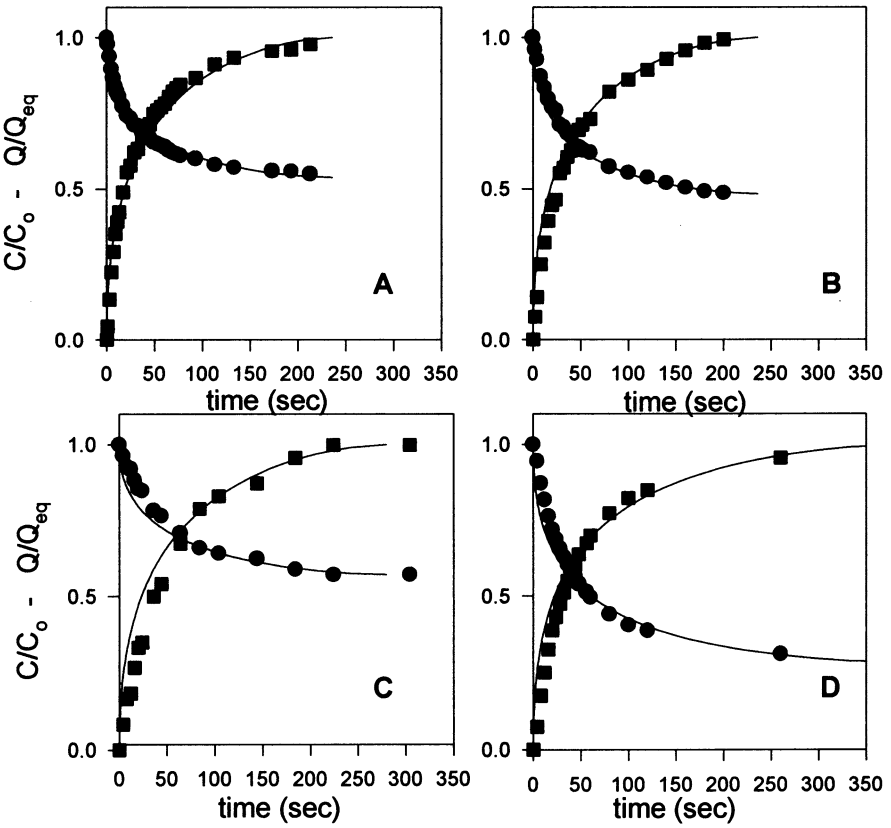

Fig. 5. Uptake of indomethacin on DEAE microspheres in 5 mM Tris–HCl buffer pH 7.4 (circle: reduced solution concentration-square: fractional uptake curve). Lines represent the pore diffusion model fitted with parameters in Table 3. (A) Starting batch solution concentration = 2.6 g/l; batch volume = 50 ml. (B) Starting batch solution concentration = 1.3 g/l; batch volume = 100 ml. (C) Starting batch solution concentration = 0.65 g/l; batch volume = 200 ml. (D) Starting batch solution concentration = 0.65 g/l; batch volume = 50 ml.

$$I_2 = \frac{1}{3R} \ln\left(\frac{\lambda^3 + \eta^3}{\lambda^3 + 1}\right) \tag{18}$$

$$\eta = \left(1 - \frac{\bar{C}(t)}{\bar{C}_\infty}\right)^{1/3} \tag{19}$$

$$\lambda = \left(\frac{1}{R} - 1\right)^{1/3} \tag{20}$$

The model assumes that film mass transfer resistance is negligible because a high stirring speed is used, the particles are spherical and instantaneous equilibrium is obtained between the solution in the pore and the surface of the solid.

The transient uptake data in Fig. 5 were fitted to the pore diffusion model, Eq. (16), allowing for determination of a pore diffusion coefficient for each set of conditions. The resulting values of pore diffusivity are summarized in Table 4. Fig. 5 indicates that the uptake was quite rapid with essentially complete saturation achieved within a 1–6 min range. Reasonable agreement between the experimental data and the model was obtained with a pore diffusion coefficient value in the 2–5.5×10^{-10} m^2/s range. These data are between 17 and 47 times smaller than the estimate of indomethacin free aqueous solution diffusivity (9.4×10^{-9} m^2/s) determined with the equation of Wilke and Chang (Wilke and Chang, 1955). The hindrance factor of diffusivity in the porous polymeric materials was within ranges previously reported (Guiochon et al., 1994).

Table 4
Parameters for stirred tank adsorption of indomethacin on DEAE microspheres

Initial concentration (g/l)	Batch volume (ml)	Pore diffusion coefficient (m^2/s)
2.60	50	2.1×10^{-10}
1.30	100	4.3×10^{-10}
0.65	200	5.5×10^{-10}
0.65	50	5.3×10^{-10}

Based on the value of pore diffusivity, estimates of kinetics of drug release could be made assuming pore diffusion as the limiting step for desorption into a finite or infinite solvent sink. Such estimates (data not shown) indicated that a very rapid drug release was obtained (within 1–5 min). Such a release profile may not be appropriate when sustained levels of drug bioactivity is sought. However, it should be pointed out that drug release mechanisms in vivo in a vascular environment are diffusion limited due the inherent hydrodynamic conditions. The absence of flow of physiological liquid will impact the release from microparticles and result in a slower release compared to the ideal in vitro well stirred tank conditions.

The models used in this work provided valuable insights into the mechanism of drug binding and elution on ion-exchange microspheres. The effect of counterions was explicitly included in the model, therefore the capacity of the bead could be assessed in various conditions. Such models can be used to characterize or select microspheres designed for specific controllable drug release. It can also be used to design new microspheres by providing information on optimal binding affinity and capacity.

Appendix A. Nomenclature

α	size exclusion fraction
β	effective charge of the solute
ε_0	interparticle porosity of packed bed column
ε_p	microspheres porosity
ε_T	total column porosity
γ	degree of ionization of the microspheres
λ	variable defined by Eq. (20)
η	variable defined by Eq. (19)
Λ	total number of charge per unit volume of bead
C	solute concentration in the liquid phase
C_0	initial solute concentration in the liquid phase
$\bar{C}_{max}$	Langmuir equation constant
$\bar{C}_\infty$	final solute concentration in the microspheres
$\bar{C}$	amount of solute adsorbed per unit volume of microspheres
D_p	pore diffusion coefficient
H	microsphere volume to liquid phase volume ratio
I	counterion concentration in the liquid phase
I_1	variable defined by Eq. (17)
I_2	variable defined by Eq. (18)
I_t	total number of counterions adsorbed per unit volume of resin
$\bar{I}$	counterion concentration adsorbed and available for exchange in the microsphere
$\hat{I}$	counterion concentration sterically excluded from ion-exchange in the microsphere
K_{eq}	apparent equilibrium constant of the ion exchange reaction
K_L	Langmuir association constant
k_{ads}, k_{des}	association and dissociation rate constants
Q	amount solute held in the column
Q_0	amount of solute held in the system (void volume)
Q_p	amount of solute held in the total porosity of the column
r	microspheres radius
R	fraction of solute ultimately bound to the microspheres
t	time
$V_{50\%}$	column effluent volume at which $C = 0.5 \times C_0$.

V_b column effluent volume at which $C = C_0$

V_c packed bed column volume

References

Altman, J.L., Dulas, D., Bache, J., 1992. Effect of cyclooxygenase blockade on blood flow through well-developed coronary collateral vessels. Circ. Res. 70, 1091–1098.

Beaujeux, R., Laurent, A., Wassef, M., lmkjh, R., 1991. Calibrated sphere embolization of craniofacial tumors and AVMs. Neuroradiology 33, 562–564.

Beaujeux, R., Laurent, A., Wassef, M., Casasco, A., Gobin, Y., Aymard, A., Rufenacht, D., Merland, J., 1996. Trisacryl gelatin microspheres for therapeutic embolization. II: Preliminary clinical evaluation in tumors and arteriovenous malformations. AJNR 17, 541–548.

Biondi, A., Merland, J.J., Reizine, D., Mijoh, L., 1990. Embolization with particles in thoracic intramedullary arteriovenous malformations: long term angiographic and clinicals results. Radiology 177, 651–658.

Brooks, C.A., Cramer, S.M., 1992. Steric mass action ion exchange: displacement profiles and induced salt gradients. AIChE J. 38, 1969–1978.

Djiandjian, R.J., Cophignon, M., Röesch, J., Iuli, P., 1973. Superselective arteriography embolization by the femoral route in neuroradiology: study of 60 cases. Neuroradiology 6, 132–145.

Farag, Y.H., Nairin, J.G., 1988. Rate of release of organic carboxylic acids from ion-exchange resins. J. Pharm. Sci. 77, 872–875.

Guiochon, G.H., Golshan-Shirazi, S.W., Katti, A.M., 1994. Fundamentals of Preparative and Non Linear Chromatography. Academic Press, New York.

Hall, W.A., Oldfield, E.H., Doppman, J.L., 1989. Recanalization of spinal arteriovenous malformations following embolization. J. Neurosurg. 70, 714–720.

Johnson, M.L., Faunt, L.M., 1992. Numerical computer methods. In: Brand, L., Johnson, M.L. (Eds.), Methods in Enzymology. Academic Press, San Diego, pp. 1–37.

Jones, C.A., Burton, M.A., Gray, B.N., 1989. In vitro release of cytotoxic agents from ion exchange resins. J. Controlled Release 8, 251–257.

Lanman, T., Martin, N., Vinters, H., 1988. The pathology of encephalic arterio-venous malformations treated by prior embolotherapy. Neuroradiology 30, 1–10.

Laurent, A., Beaujeux, R., Wassef, M., Rufenacht, D., Boschetti, E., Merland, J.J., 1996. Trisacryl gelatin microspheres for therapeutic embolization, I: Development and in vitro evaluation. AJNR 17, 533–540.

LeVan, D.M., Carta, G., Yan, C.M., 1997. Adsorption and ion exchange. In: Perry, R. (Ed.), Perry's Chemical Engineers' Handbook. Mc Graw-Hill, New York, pp. 16–66.

Li, Q.W., Grandmaison, E.W., Hsu, C.C., Taylor, D.H., Goosen, M.F., 1995. Interparticle and intraparticle mass-transfer in chromatographic separation. Bioseparation 5, 189–202.

Marquardt, D.W., 1963. An algorithm for least square estimation of non-linear parameters. J. Soc. Ind. Appl. Math. 11, 431–441.

Mohamed, F.A., 1996. Use of Dowex-X2 ion exchange resin for preparation of sustained release diclofenac delivery system I. Preparation and release studies. STP Pharma Sci. 6, 410–416.

Niechajev, I., Clodius, I., 1990. Histologic investigation of vascular malformations of the face after transarterial embolization with ethibloc and other agents. Plastic Recons. Surg. 86, 664–671.

Ruthven, D.M., 1984. Principles of Adsorption and Adsorption Processes. Wiley, New York.

Theo, N.K., Ruthven, D.M., 1986. Adsorption of water from aqueous ethanol using 3 A molecular sieves. Ind. Eng. Chem. Process. Des. Dev. 25, 17–21.

Thomashefski, J.H., Cohen, A.W., Doershuk, C., 1988. Long term histo-pathologic follow-up of bronchial arteries after therapeutic embolization with polyvinyl alcohol in patients with cystic fibrosis. Hum. Pathol. 19, 555–561.

Vinters, H., Lundie, M., Kaufmann, J.H., 1986. Longterm pathological follow-up of cerebral arteriovenous malformations treated by embolization with bucrylate. N. Engl. J. Med. 314, 477–483.

Whitley, R.D., Wachter, R., Liu, F., Wang, L.N., 1989. Ion-exchange equilibria of lysozyme, myoglobulin and bovine serum albumin. Effective valence and exchanger capacity. J. Chromatogr. 465, 137–156.

Wilke, C.R., Chang, P., 1955. AIChE J. 1, 254.